European Journal of Medicinal Chemistry 50 (2012) 154–162

Contents lists available at SciVerse ScienceDirect

European Journal of Medicinal Chemistry

journal homepage: http://www.elsevier.com/locate/ejmech

Original article

Design, synthesis, theoretical calculations and biological evaluation of new non-symmetrical choline kinase inhibitors

Belén Rubio-Ruíz [a], Ana Conejo-García [a], Pablo Ríos-Marco [b], María Paz Carrasco-Jiménez [b], Josefa Segovia [b], Carmen Marco [b], Miguel A. Gallo [a], Antonio Espinosa [a], Antonio Entrena [a,*]

[a] Departamento de Química Farmacéutica y Orgánica, Facultad de Farmacia, Campus de Cartuja, 18071 Granada, Spain
[b] Departamento de Bioquímica y Biología Molecular I, Facultad de Ciencias, Campus de Fuentenueva, 18071 Granada, Spain

ARTICLE INFO

Article history:
Received 9 September 2011
Received in revised form
17 January 2012
Accepted 24 January 2012
Available online 3 February 2012

Keywords:
Antiproliferative agents
Choline kinase inhibitors
Pyridinium compounds
Molecular modeling
Docking studies

ABSTRACT

Inhibition of Choline Kinase (ChoK) has been reported as a therapeutical target in the treatment of some kinds of tumor. In this paper, the design and synthesis of new non-symmetrical monocationic ChoK inhibitors is described, bearing a cationic head and an adenine moiety connected by linkers of different lengths. Docking studies indicate that the cationic head of these compounds could be inserted into the choline binding site of the enzyme, while the adenine moiety could be stabilized into the ATP binding site. Docking studies also support the difference of activity of the synthesized compounds, which depends on both the substituent at position 4 of the cationic head and the linker length, being dimethylamine and 1,4-diphenylbutane respectively, the most appropriate ones. Compounds **14** ($IC_{50} = 10.70 \pm 0.40$ μM) and **17** ($IC_{50} = 6.21 \pm 0.97$ μM) are the most potent ChoK inhibitors and suitable for further modification with a view to obtain more potent antitumor compounds.

1. Introduction

Choline (Cho) is phosphorylated by choline kinase (ChoK) to generate phosphocholine (PCho), which represents the first step in the biosynthesis of a membrane phospholipid, phosphatidylcholine [1]. During the tumor formation the phospholipid metabolism is altered, which consequently leads to an increase in the PCho levels [2,3] associated with the overexpression of ChoK. Platelet-derived, epidermal, insulin dependent and vascular endothelial growth factors enhance the ChoK activity during the tumor production [4]. In addition, several oncogenes such as *ras* or *rhoa* increase ChoKα activity resulting in higher intracellular levels of PCho [5,6]. Recently it has been observed that hypoxia can induce ChoK expression in cancer cells [7]. Thus, an activation of ChoK and the resulting increase in PCho levels have been proposed as necessary events for the proliferation of certain cell types [8].

In mammalian cells, the three known isoforms of ChoK (ChoKα1, ChoKα2, and ChoKβ) are encoded by two genes: *chokα* and *chokβ*. None of the isoforms are active as monomers and the active enzyme consists of homo- or heterodimers [1]. Recent studies on the biological function of ChoK isozymes revealed that ChoKα may play a more prominent role in cancer development as compared to ChoKβ, as only ChoKα was upregulated in breast cancer cell lines [9] and specific depletion of the ChoKα isoform by shRNA selectively induced apoptosis in several tumor-derived cell lines without affecting the viability of normal primary cells [10]. The ChoKα isoform has also been proposed as a new prognostic marker for predicting the clinical outcome in patients with non-small-cell lung cancer [11]. These observations have resulted in the development of an antitumoral strategy focused on ChoK inhibition.

The synthesis of several derivatives was based on structural modifications of Cho uptake inhibitor hemicholinium-3 (**HC-3**, Fig. 1). We have previously reported a series of compounds namely bis-pyridinium (**1**–**3**) [12], bis-quinolinium (**4**) [13], tris-pyridinium (**5**) [14], cyclophanes (**6**) [15,16] and bicyclophanes (**7**) [17] as ChoK inhibitors. All these compounds show a symmetrical structure, bearing two or three cationic heads connected through a linker.

Our research group prepared a homology model of the human choline kinase isoform ChoKα [18] based on the 3D structure of *Caenorhabditis elegans* choline kinase (CKA2 PDB id: 1NW1) [19]. In

Abbreviations: Cho, choline; ChoK, choline kinase; PCho, phosphocholine; HC-3, hemicholinium-3; PHC-3, phosphohemicholinium-3; CKA2, Caenorhabditis elegans choline kinase; SAR, structure–activity relationship; HepG2, human hepatocellular carcinoma; FBS, fetal bovine serum; MEM, minimal essential medium; MD, molecular dynamic; SFXC, surflex-dock geomx; LDH, lactate dehydrogenase.

* Corresponding author. Tel.: +34 958 243848; fax: +34 958 243845.
E-mail address: aentrena@ugr.es (A. Entrena).

0223-5234/$ – see front matter © 2012 Elsevier Masson SAS. All rights reserved.
doi:10.1016/j.ejmech.2012.01.050

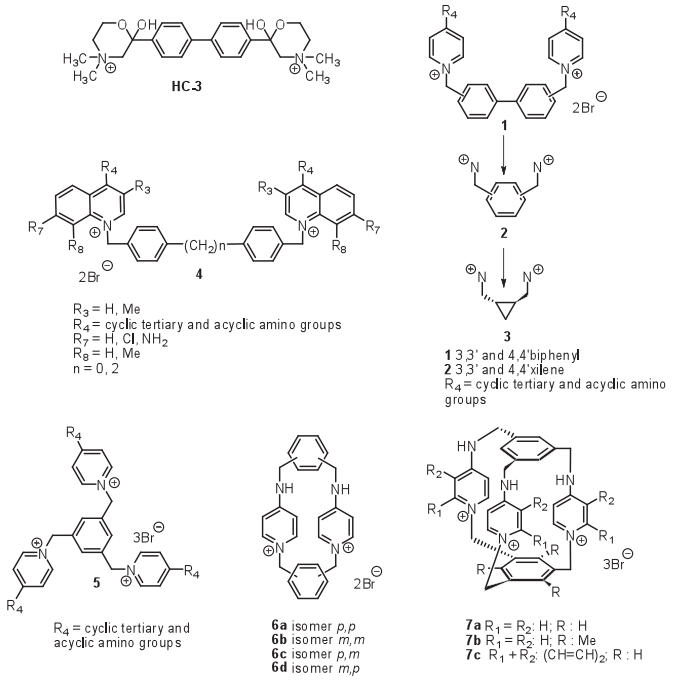

Fig. 1. Chemical structures of bis- and tris-quaternary ammonium salts **1**–**7**.

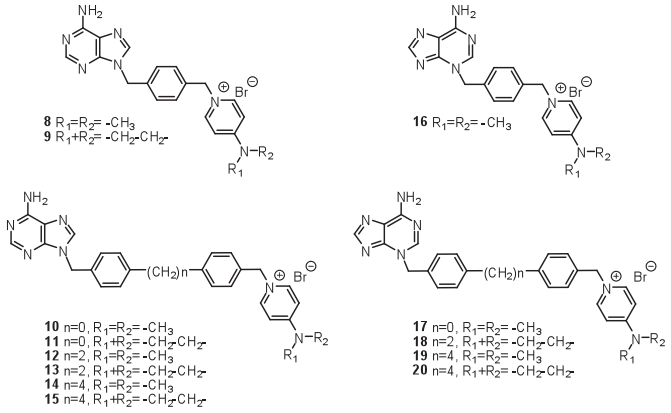

Fig. 2. Chemical structures of mono-quaternary pyridinium salts **8**–**20**.

that paper, preliminary docking studies of some of our previously synthesized ChoK inhibitors were also included. It was observed that the size of symmetrical biscationic inhibitors is appropriated to bind simultaneously in both the ATP and choline putative binding sites of the protein model (Fig. S1, Supplementary data).

Simultaneously to the publication of our ChoKα homology model, the crystal structure of human ChoKα2 isoform was published [20]. Three crystal structures corresponding to the *apo* form (PDB id: 2CKO) and two complexes with the products of the enzymatic reaction, ADP (PDB id: 2CKP) and PCho (PDB id: 2CKQ) were described in this paper. These structures allow the correct identification of both the ATP and Cho binding pockets (Fig. S2).

The preliminary docking studies performed on the homology model, and the fact that the nature of the residues that constitute the ATP binding site is quite different to those residues that form the Cho binding site, suggested the idea of preparing non-symmetric monocationic inhibitors that could bind in both binding sites. Such inhibitors should conserve one cationic head that could be inserted into the Cho binding site, but the second cationic head will be substituted by another fragment that could mimic the ATP adenine moiety.

In this paper, the first family of these new inhibitors is presented (Fig. 2). In these compounds, adenine itself was used to mimic the ATP adenine moiety, and 4-dimethylamino- or 4-pyrrolidino-pyridinium salts were used as cationic head. Both fragments are separated by several linkers that have been chosen to study the influence of the linker size in the inhibition of ChoK.

2. Results

2.1. Chemistry

Four different types of linkers have been used, benzene, biphenyl, 1,2-diphenylethane and 1,4-diphenylbutane, that are bisbromomethylated in the adequate position in order to insert both the adenine and the cationic head. 1,4-Bis(bromomethyl) benzene is commercially available. Reaction between biphenyl or 1,2-diphenylethane with formaldehyde and hydrogen bromide in the presence of H_3PO_4 yields 4,4′-bis(bromomethyl)biphenyl [21] and 4,4′-bis(bromomethyl)bibenzyl [22], respectively. Finally, 1,4-Bis[4-(bromomethyl)phenyl]butane was prepared by reduction of *trans,trans*-1,4-diphenyl-1,3-butadiene with Pd/C in glacial acetic acid, followed by the bisbromomethylation in the previous mentioned conditions [22].

The synthesis of the target molecules **8**–**20** has been carried out as described in Scheme 1. Reaction between the appropriate bisbromomethylated linker and the adequate pyridine derivative in butanone, at room temperature during 3 h, yields the intermediates **21**–**28**. ^{1}H NMR of the crude reaction showed the presence of the bisquaternisation structures as side products which have to be separated from the monocationic intermediates by filtration and thorough washing with butanone, ethyl acetate and diethyl ether or flash column chromatography on silica gel using CH_2Cl_2/MeOH (10/0.5) as eluent (see experimental protocols for details).

The reaction between the intermediates **21**–**28** and the purine moiety was carried out in DMF using K_2CO_3 as a base. The reaction mixture was microwave-irradiated at a temperature of 130 °C for 30 min. The preferential N-9 substitution on adenine was accompanied by formation of the corresponding N-3 isomers. In general the formation ratio of the N-9:N-3 isomers is 1.5:1, except for **15** in which the ratio has shown to be reversed (1:1.5). When the total yield of the N-3 isomer is smaller than 10% it was no possible to isolate these structures (N-3 isomers of **9**, **11** and **12**).

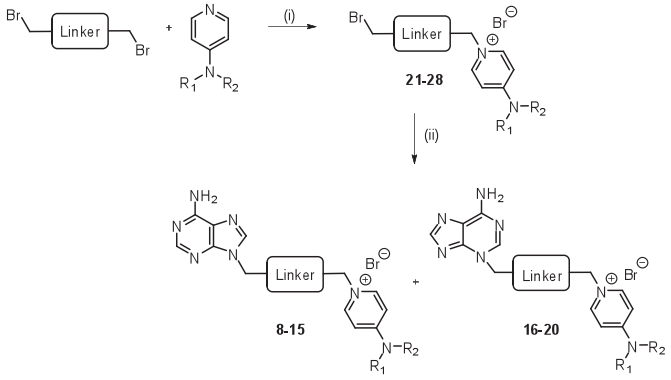

Scheme 1. Synthesis of the N-9 and N-3 mono-quaternary pyridinium salts **8**–**20**. Reagents and conditions: i) Butanone, rt, 3 h; ii) Adenine, K_2CO_3, DMF, 130 °C, MW, 30 min.

2.2. Pharmacology

Compounds **8**–**20** were tested in an *in vitro* system using human ChoK as a target. This assay allows the evaluation of the affinity of the compounds for ChoK without considering the possible passage through biological membranes. The effects on cell proliferation by the ChoK inhibitors were also investigated on the human hepatoma HepG2 cell line. Because of their high degree of morphological and functional differentiation *in vitro*, HepG2 cells are a suitable model for the search of new antitumor drugs. Two initial assays were performed for each molecule using a final concentration of 10 μM and 50 μM, with the object of identifying the more potent compounds. IC_{50} values for ChoK inhibition and antiproliferative activity were also measure for selected compounds obtained in the initial assays by using the ED50plus v1.0 software. The activity in the antiproliferative assay reflected not only their affinity for the enzyme but also other properties like the capacity of the compound to pass trough the cell membrane.

Table 1 shows the ChoK inhibition and the antiproliferative activity for **8**–**20**. The differences in the enzyme inhibition of each N-9 derivative and the corresponding N-3 regioisomer are not too much significant and the antiproliferative activity between the N-9 and the corresponding N-3 derivative are similar too. The biological effect is dependent on the linker length although a clear structure–activity relationship between the size of this moiety and the inhibition of ChoK and/or the HepG2 antiproliferative activity is not observed. The most potent ChoK inhibitor of the N-9 series is compound **14** that presents as a linker a 1,4-diphenylbutane group and shows an $IC_{50} = 10.70 \pm 0.40$ μM. The antiproliferative IC_{50} of **14** measured on HepG2 cell line gives a value of 49.70 ± 1.78 μM.

IC_{50} ChoK inhibition value has also been calculated for the most active compound belonging to the N-3 series (**17**, IC_{50} ChoK $= 6.21 \pm 0.97$ μM). The most potent structure as antiproliferative agent of this series is compound **19** that presents an IC_{50} value of 38.9 ± 1.02 μM.

In general the dimethylamine substituent at position 4 of the pyridinium fragment lead to higher ChoK inhibitory potency. In the N-9 series, compounds **8**, **12** and **14** show higher inhibition percentage than compounds **9**, **13** and **15**, respectively, with the only exception of compound **11** that presents a pyrrolidine group and is more potent than **10**. Unfortunately, in the N-3 series some compounds could not be isolated and this relationship between the dimethylamine and pyrrolidine derivatives can not be confirmed, except for **19** bearing a dimethylamine substituent which is more potent than compound **20.**

Regarding the antiproliferative activity, in the N-9 series can be observed that the 4-pyrrolidine derivatives (**9**, **11**, **13** and **15**) show a slightly higher antiproliferative activity than the corresponding dimethylamine analogs (**8**, **10**, **12** and **14**) probably due to the higher lipophilicity of these structures as a consequence of the presence of two additional methylene groups in the 4-pyrrolidine derivatives that allows a better penetration into HepG2 cells. Finally, in the N-3 series, compounds **19** and **20** show a similar antiproliferative activity, and no other relationships can be established due to the lack of several derivatives of this series.

The index of cytotoxicity used in this study was the measurement of lactate dehydrogenase (LDH) leakage [23]. Toxicity was only apparent after treatment with 50 μM of **15** (data not shown). For the rest of the compounds the decrease in cell number observed after 24 h of treatments was not related to any acute cytotoxicity produced by plasma membrane leakage since we did not detect cytotoxicity determined by measurements LDH leakage.

Table 1
ChoK inhibition and HepG2 antiproliferative activity for the target compounds **8**–**20**.

Comp.	Inhib.ChoK (%)		Antiprolif. (%)	
	10 μM	50 μM	10 μM	50 μM
8	46.7 ± 0.9	54.1 ± 2.7	0	5.1 ± 0.7
9	0	27.0 ± 2.8	0	15.5 ± 0.5
10	37.6 ± 0.4	51.0 ± 2.5	0	10.3 ± 0.6
11	50.2 ± 3.9	72.8 ± 2.9	10.4 ± 1.0	45.0 ± 2.2
12	38.6 ± 4.2	81.0 ± 1.7	10.5 ± 1.5	10.5 ± 0.7
13	28.6 ± 2.7	46.9 ± 3.7	30.1 ± 2.2	45.0 ± 4.2
14	66.7 ± 3.8	89.7 ± 3.1	10.2 ± 1.8	45.5 ± 2.5
15	36.9 ± 3.8	41.9 ± 3.3	15.4 ± 2.8	90.1 ± 1.6
16	25.0 ± 3.4	50.2 ± 2.9	10.3 ± 1.7	2.5 ± 0.3
17	62.3 ± 3.5	71.4 ± 2.1	10.0 ± 1.9	7.0 ± 0.4
18	0.1 ± 0	24.8 ± 3.1	11.6 ± 1.8	30.0 ± 2.1
19	61.3 ± 2.8	68.2 ± 2.4	14.3 ± 1.3	56.1 ± 0.7
20	22.6 ± 3.6	59.9 ± 3.3	13.7 ± 1.1	46.5 ± 2.1

2.3. Molecular modeling and docking studies

Recently the 3D structure of both human ChoKα1 (PDB id: 3G15) and ChoKβ (PDB id: 3FEG) isoforms in complex with **HC-3**, the first known inhibitor of this enzyme, has been published [24]. In the crystal structure of ChoKα1 both **HC-3** and ADP are present, while in the ChoKβ structure **HC-3** is present in a phosphorilated form (PHC-3), since it was phosphorilated during the crystallization process [24].

Human choline kinase ChoKα1 (PDB id: 3G15) was chosen for the docking studies by two reasons: i) ChoKα1 isoform is overexpressed in a large number of human tumors, playing a key role in the carcinogenic process, while the role of ChoKβ is still not so clear [25]; and ii) In this crystal structure both the **HC-3** inhibitor and ADP are presents. Molecular modeling studies were performed using Sybyl-X program [26].

Docking studies indicate that there are different modes for the binding of the inhibitors inside the enzyme. The length of the linker in compounds **8** and **9** (and also **16**) is too short to allow these molecules to be allocated in both ATP and Cho binding sites simultaneously. The obtained poses for these compounds indicate that they can be inserted into the Cho binding site or into the ATP binding site.

Fig. 3 shows as an example the poses obtained for compounds **8** and **9**. The cationic head of compound **8** is inserted into the hydrophobic pocket of the Cho binding site and is stabilized by

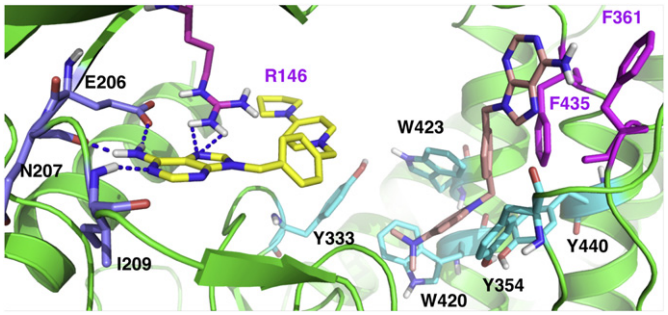

Fig. 3. The most stable poses obtained for compounds **8** (right, carbon atoms in orange color) and **9** (left, carbon atoms in yellow color) in the docking studies. The pyridinium moiety of compound **8** is inserted into the hydrophobic pocket of the Cho binding site (Tyr333, Tyr354, Tyr440, Trp420 and Trp423, carbon atoms in cyan color), while the phenyl and the adenine moieties are stabilized by a π-π interaction with Phe435 and Phe361 (magenta). Compound **9** is inserted into the ATP binding site (Glu206, Gln207 and Ile209, carbon atoms in blue slate color), being the adenine moiety stabilized by three H-bonds with these residues and by two additional H-bonds with Arg146 (carbon atoms in magenta color). (For interpretation of the references to color in this figure legend, the reader is referred to the web version of this article.)

means of π-cation interactions, and the phenyl ring is stabilized by a π-π interaction with Phe435. The adenine moiety points toward the surface of the protein and is parallel to Phe361, making a π-π interaction with this residue. This pose can be superimposed to the **HC-3** inhibitor inserted into the crystal structure of the enzyme (Fig. S3). A similar pose has been obtained for compound **9** (Fig. S4), but the higher volume of the 4-pirrolidine substituent in relation to the 4-dimethylamine of compound **8** prevents a correct orientation of the molecule inside the Cho binding site, and the interaction between the benzene moiety and Phe435 does not exist in compound **9**.

In the most stable pose of compound **9**, the molecule is inserted into the ATP binding pocket, and is stabilized by hydrogen bonds between the adenine moiety and Ile209, Asn207, Asp206 and Arg146 (Fig. 3). The adenine moiety can be superimposed with the ADP adenine that is present in the crystal structure of the enzyme (Fig. S5). No similar pose has been obtained for compound **8**, probably because the union to the Cho binding site is more favored.

On the other hand, compounds **10**–**15** bear longer linkers, whose length is enough to allow these molecules to bind simultaneously in both ATP and Cho binding sites. Fig. 4a shows as an example the best poses obtained for compounds **11**, **13** and **15**. It can be observed that the adenine moiety of the three compounds is situated on the ATP binding site, performing hydrogen bonds interactions with Ile209 and Asn207, similarly to the interactions between the ADP and the ChoKα1 in the crystal structure of the complex (PDB id: 3G15). The cationic head of these molecules is inserted into the Cho binding site, with the 4-pyrrolidinopyridinium moiety parallel to Trp423. The proximity of both fragments stabilizes the inhibitor inside the hydrophobic pocket by means of π-π or π-cation interactions. The linker of compounds **11** and **13** can adopt an extended conformation and their main poses for both molecules are almost parallels each other, being the cationic head of compound **13** slightly near to Trp423. The longer linker of compound **15** made this molecule to adopt a more folded conformation, and the cationic head adopts a different disposition into the Cho binding site in comparison with those of compounds **11** and **13**. Figures S6 and S7 show a more detailed view of the pose of each molecule.

Regarding N-3 derivatives, the overall behavior of these molecules is similar to that of N-9 derivatives. Compound **16** and the N-3 isomer of compound **9** have a short linker and can only occupy one of the binding sites, the ATP or the Cho binding site. Compound **16** shows a similar pose to that of compound **8** inside into the Cho binding site, with the benzene moiety interacting with Phe345 trough a π-π interaction. The N-3 isomer of **9** is inserted into the ATP binding site, and established hydrogen bonds with Ile209, Asn207 and Glu246. The main difference with the pose of compound **9** is that the adenine moiety is rotated and adopts an opposite orientation in relation to the ADP adenine observed in the crystal structure. Figure S8 and S9 show the two main poses of both compounds.

Like compounds **10**–**15**, compounds **17**–**20** (and the non isolated N-3 isomers of **11** and **12**) have a longer linker and can be accommodated simultaneously in both ATP and Cho binding sites. Fig. 4b shows as an example the main poses obtained for **17** and for compound **20**. In this case, the orientation of the adenine moiety of **17** adopts an orientation similar to that described for the N-3 isomer of compound **9** Fig. S9), rotated in an opposite direction to the ADP adenine fragment. This orientation seems to be necessary since the linker is connected to N-3 atom and the length of the linker is not enough to allow the insertion of the cationic head into the Cho binding site when the adenine adopts an orientation similar to that of the ADP adenine.

Compound **20** shows an adenine orientation similar to the N-9 derivatives above described. In this case, the length of the linker of compound **20** is higher and allows the cationic head to be inserted into the Cho binding site. Even more, the linker is less folded than in compound **15**. Figures S10 and S11 show a more detailed view of the pose of each molecule.

3. Discussion

N-9 derivatives **8**–**15** were designed as new monocationic inhibitors of ChoK. Nevertheless, during the synthesis of these molecules, N-3 derivatives **16**–**20** were also obtained as subproducts of the synthetic reactions, and their biological activity as ChoK inhibitors were also evaluated.

Biological assays were performed at two different concentrations: 10 and 50 μM in order to determine the more potent ChoK inhibitors. The IC_{50} values were measured only for the most potent compounds of each series (**14** and **17**).

Among N-9 derivatives, and regarding the ChoK inhibition, some structure relationships can be established. It can be observed that the inhibition activity depends on both the nature of the cationic head and the length of the linker. Compounds bearing a 4-dimethylaminopyridinium moiety as a cationic head are more potent inhibitors when the molecules bear a benzene, 1,2-diphenylethane or 1,4-diphenylbutane linker, while 4-pyrrolidinopyridinium moiety originates more potent inhibitors only when a biphenyl fragment is the linker of the inhibitor.

In compounds **8** and **9**, with the benzene linker, the higher activity of the 4-dimethylaminopyridinium derivative (**8**) can be easily explained in base to the preferred poses obtained for this molecule. In the preferred pose for **8,** the cationic head is inserted into the Cho binding site, and is stabilized by a π-π interaction between the benzene moiety of the linker and Phe435 that adopts a parallel orientation each other (Fig. 3). Nevertheless, the

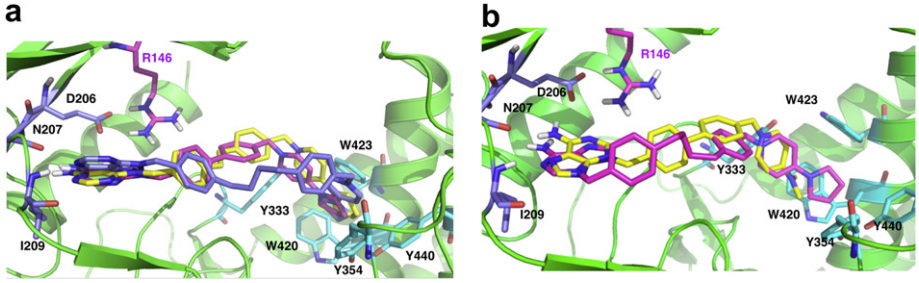

Fig. 4. (a) The most stable poses obtained in the docking studies of compounds **11** (magenta), **13** (yellow) and **15** (blue) inside the ChoKα1. (b) The most stable poses obtained in the docking studies of compounds **17** (yellow), and **20** (magenta) inside the ChoKα1. All compounds are simultaneously situated inside both ATP and Cho binding sites. Adenine moieties adopt an opposite orientation in each compound to allow the cationic head to be inserted into the Cho binding site. (For interpretation of the references to color in this figure legend, the reader is referred to the web version of this article.)

equivalent pose of compound **9** into the Cho binding site is not stabilized by such type of interaction (Fig. S4) due to the higher volume of the 4-pyrrolidine substituent that prevents the correct orientation of the ligand inside the Cho binding site. In fact, in the most stable pose obtained for compound **9**, the inhibitor is inserted into the ATP binding site, and not in the Cho binding site. This difference could be the explanation of the higher inhibition activity of compound **8** in relation to compound **9**: compound **8** binds more efficiently inside the Cho binding site.

In compounds **10** and **11**, the biphenyl linker is long enough to allow the insertion of the adenine moiety into the ATP binding site and of the cationic head into the Cho binding site. In this pair of compounds, the 4-pyrrolidinopyridinium cationic head gives place to a more potent inhibitor. This could be due to the smaller volume of the dimethylamine substituent. The depth of the insertion of both cationic head inside the hydrophobic pocket is similar and the length of the linker controls it. Nevertheless, in compound **10** the cationic head is smaller and it can be situated nearer to Tyr354 and slightly far to Trp423 (6.6 Å). In compound **11**, the higher volume of the pyrrolidine moiety brings the cationic head closer to Trp423 (4.3 Å), originating a more potent π-π interactions between the cationic head of compound **11** with Trp423. This could be the reason for the higher activity of compound **11** in relation to compound **10** (Fig. 5a).

In compounds **12**–**15**, the length of the linker is higher, and consequently, allows a more flexible orientation of the cationic head inside the Cho binding site. Fig. 5b shows as an example the difference in the orientation of the cationic head in compounds **14** and **15**. In these molecules the linker is very long and must be folded to allow the accommodation of the adenine and the cationic head. Nevertheless, in compound **14**, the smaller volume of the dimethylamine substituent allows a more deep insertion of the cationic head inside the hydrophobic pocket of the Cho binding site. A similar situation occurs in compound **12** and **13**. The longer length of the linker and the smaller volume of the dimethylamine moiety in compounds **12** and **14** allow a deeper insertion of the cationic head inside the hydrophobic pocket of the Cho binding site, and this fact could be an explanation of the higher activity of these molecules in relation to their corresponding compounds **13** and **15**, respectively.

The differences in activity of the N-3 derivatives in relation to their corresponding N-9 analogs is really smaller. Furthermore, since some of these molecules could not be isolated, the structure–activity relationships (SAR) cannot be completely established, but docking studies indicates similar preference for the ATP and/or choline binding sites. Only compounds **19** and **20** can be compared and their inhibition activity is similar to that of compounds **14** and **15**. This fact is expected since the linker and the cationic head are similar in these molecules.

Regarding antiproliferative activity (Table 1), the SAR can be hardly established, since it depends not only on the affinity of these molecules as ChoK inhibitors, but also on their facility to pass trough the membrane cells. In general, it can be observed that 4-pyrrolidine derivatives show a slightly higher activity than the corresponding dimethylamine analogs. This fact could be due to the higher lipophilicity of these molecules due to the presence of two additional carbon atoms. On the other hand, it can also be observed that compounds with longer linker also show higher antiproliferative activity and this could also be due to their higher lipophilicity.

4. Conclusions

Compounds described on this paper present inhibitory activity against ChoK. Docking studies indicate that in most cases, these molecules could bind simultaneously in both ATP and Cho binding sites of this enzyme, except when the linker is a benzene moiety. The adenine moiety binds into the ATP binding site in a similar mode to the ADP adenine fragment present in the crystal structure of the ChoK/ADP/**HC-3** complex. In general, 4-dimethylaminopyridinium moiety acts as a better cationic head since it permits a better insertion inside the Cho binding site. Only when the linker is a biphenyl fragment, the 4-pyrrolidinopyridinium is better as a cationic head. Unfortunately, a direct relationship between the inhibition of ChoK and the antiproliferative activity has not been found. Nevertheless, these molecules could serve as a pattern for the design of new and more potent ChoK inhibitors.

5. Experimental protocols

5.1. Chemistry

Melting points were taken in open capillaries on a Stuart Scientific SMP3 electrothermal melting point apparatus and are uncorrected. Elemental analyses were performed on the Thermo Scientific Flash 2000 analyzer only on the final compounds tested as ChoK inhibitors. The measured values for C, H, and N agreed to within ±0.40% of the theoretical values. Analytical thin-layer chromatography (TLC) was performed using Merck Kieselgel 60 F_{254} aluminum plates and visualized by UV light or iodine. All evaporation was carried out in vacuo with a Büchi rotary evaporator and the pressure controlled by a Vacuubrand CVCII apparatus. For flash chromatography, Merck silicagel 60 with a particle size of 0.040–0.063 mm (230–400 mesh ASTM) was used. Nuclear magnetic resonance spectra were recorded on a 500 MHz ^{1}H and 125 MHz ^{13}C NMR Varian NMR-System-TM 500, a 400 MHz ^{1}H NMR Varian NMR-System-TM 400 or 300 MHz ^{1}H and 75 MHz ^{13}C NMR

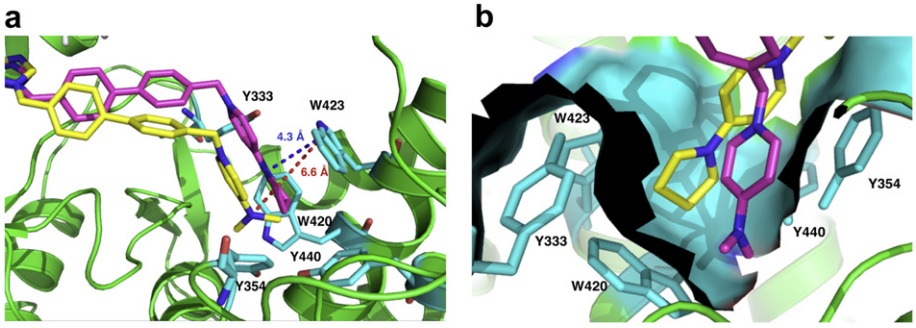

Fig. 5. (a) Comparison between the most stable poses obtained for compounds 10 (yellow) and 11 (magenta). The cationic head of compound **11** is situated near to Trp423. (b) Detailed view of the cationic heads of compounds **14** (magenta) and **15** (yellow) inserted into the hydrophobic pocket of the Cho binding site. The cationic head of compound **14** can be inserted more deeply inside the hydrophobic pocket. (For interpretation of the references to color in this figure legend, the reader is referred to the web version of this article.)

Varian Inova-TM spectrometers at ambient temperature. Chemical shifts (δ) are quoted in parts per million (ppm) and are referenced to the residual solvent peak. Spin multiplicities are given as s (singlet), bs (broad singlet), d (doublet), t (triplet), q (quintuplet) and m (multiplet). High-resolution Nano-Assisted Laser Desorption/Ionization (NALDI-TOF) or Electrospray Ionization (ESI-TOF) mass spectra were carried out on a Bruker Autoflex or a Waters LCT Premier Mass Spectrometer, respectively. Microwave-assisted synthesis was carried out in an Initiator 2.0 single-mode microwave instrument producing controlled irradiation at 2.450 GHz (Biotage AB, Upsala). Reaction time refers to hold time at 130 °C, not to total irradiation time. The temperature was measured with an IR sensor on the outside of the reaction vessel. All compounds were dried at 40 °C and 0.1 mmHg for 24 h, but many held on tenaciously to water which appear to be solvates. Adenine, 4-(pyrrolidino)pyridine, 4-(*N*,*N*-dimethylamino)pyridine and 1,4-bis(bromomethyl)benzene were purchased from Aldrich. 4,4′-Bis(bromomethyl)biphenyl [21], 4,4′-bis(-bromomethyl)bibenzyl [22] and 1,4-bis[4-bromomethyl)phenyl] butane [22] were synthesized according to literature procedures.

5.2. General procedure for the synthesis of the monocationic intermediates

A butanone solution (40 mL) of the linker (2 equiv.) and the corresponding 4-substituted pyridine (1 equiv.) was stirred at room temperature for 3 h **21**, **22**, **23**, **25** and **26** were isolated after filtration and thorough washing with butanone, ethyl acetate and diethyl ether. In the case of **24**, **27** and **28**, the reaction mixture was evaporated, and the crude products purified by flash column chromatography on silica gel using CH_2Cl_2/MeOH (10/0.5) as eluent.

5.2.1. 1-[4-(bromomethyl)benzyl]-4-(dimethylamino)pyridinium bromide (**21**)

Yield: 76%. M.p. 186–189 °C ^{1}H NMR (300 MHz, CD_3OD) δ 8.22 (d, J = 7.9 Hz, 2H); 7.48 (d, J = 8.2 Hz, 2H); 7.36 (d, J = 8.2 Hz, 2H); 7.01 (d, J = 7.9 Hz, 2H); 5.37 (s, 2H); 4.57 (s, 2H); 3.25 (s, 6H). ^{13}C NMR (125 MHz, DMSO-d_6) δ 155.88, 141.99 × 2, 138.54, 135.82, 129.87 × 2, 128.23 × 2, 108.01 × 2, 58.90, 39.77 × 2, 33.72. HRMS (m/z) calcd for $C_{15}H_{18}N_2Br$ $(M - Br)^+$ 305.0653; found 305.0644.

5.2.2. 1-[4-(bromomethyl)benzyl]-4-pyrrolidinopyridinium bromide (**22**)

Yield: 77%. M.p. 203 °C (gel) – 241 °C (foam). ^{1}H NMR (400 MHz, CD_3OD) δ 8.18 (d, J = 7.6 Hz, 2H); 7.48 (d, J = 8.1 Hz, 2H); 7.34 (d, J = 8.1 Hz, 2H); 6.86 (d, J = 7.6 Hz, 2H); 5.35 (s, 2H); 4.57 (s, 2H); 3.55 (t, J = 6.8 Hz, 4H); 2.12 (q, J = 6.8 Hz, 4H). ^{13}C NMR (75 MHz, CD_3OD) δ 155.18, 143.04 × 2, 140.87, 136.35, 131.11 × 2, 129.64 × 2, 109.76 × 2, 61.32, 49.74 × 2, 33.079, 26.129 × 2. HRMS (m/z) calcd for $C_{17}H_{20}N_2Br$ $(M - Br)^+$ 331. 0810; found 331.0811.

5.2.3. 1-{4-[4-(bromomethyl)phenyl]benzyl}-4-(dimethylamino) pyridinium bromide (**23**)

Yield: 70%. M.P. 209–210 °C ^{1}H NMR (400 MHz, CD_3OD) δ 8.25 (d, J = 7.5 Hz, 2H); 7.70 (d, J = 8 Hz, 2H); 7.61 (d, J = 8 Hz, 2H); 7.52–7.45 (m, 4H); 7.02 (d, J = 7.5 Hz, 2H); 5.41 (s, 2H), 4.62 (s, 2H), 3.26 (s, 6H). ^{13}C NMR (75 MHz, CD_3OD) δ 158.00, 143.12 × 2, 142.61, 141.28, 139.33, 135.39, 130.83 × 2, 129.99 × 2, 128.88 × 2, 128.30 × 2, 109.16 × 2, 61.41, 40.39 × 2, 33.69. HRMS (m/z) calcd for $C_{21}H_{22}N_2Br$ $(M - Br)^+$ 381.0966; found 381.0964.

5.2.4. 1-{4-[4-(bromomethyl)phenyl]benzyl}-4-pyrrolidinopyridinium bromide (**24**)

Yield: 61%. M.p. 106–109 °C ^{1}H NMR (400 MHz, CD_3OD) δ 8.22 (d, J = 7.5 Hz, 2H); 7.70 (d, J = 8.1 Hz, 2H); 7.61 (d, J = 8.1 Hz, 2H); 7.50 (d, J = 8.1 Hz, 2H); 7.45 (d, J = 8.1 Hz, 2H); 6.87 (d, J = 7.5 Hz, 2H); 5.40 (s, 2H); 4.62 (s, 2H); 3.56 (t, J = 6.6 Hz, 4H); 2.12 (q, J = 6.6 Hz, 4H). ^{13}C NMR (125 MHz, CD_3OD) δ 155.03, 142.99 × 2, 142.34, 141.13, 139.25, 135.52, 130.83 × 2, 130.04 × 2, 128.78 × 2, 128.24 × 2, 109.73 × 2, 61.36, 49.86 × 2, 33.81, 26.07 × 2. HRMS (m/z) calcd for $C_{23}H_{24}N_2Br$ $(M - Br)^+$ 407.1123; found 407.1109.

5.2.5. 1-{4-[4-(bromomethyl)phenethyl]benzyl}-4-(dimethylamino)pyridinium bromide (**25**)

Yield: 74%. M.p. 242 °C (gel) – 245 °C (foam). ^{1}H NMR (300 MHz, CD_3OD) δ 8.21 (d, J = 8 Hz, 2H); 7.29–7.19 (m, 6H); 7.12 (d, J = 8.1 Hz, 2H); 6.99 (d, J = 8 Hz, 2H); 5.32 (s, 2H); 4.52 (s, 2H); 3.24 (s, 6H); 2.91 (m, 4H). ^{13}C NMR (75 MHz, CD_3OD) δ 157.99, 144.24, 143.12, 143.03 × 2, 137.31, 133.67, 130.62 × 2, 130.15 × 2, 129.91 × 2, 129.37 × 2, 109.08 × 2, 61.58, 40.28 × 2, 38.34, 38.30, 34.13. HRMS (m/z) calcd for $C_{23}H_{26}N_2Br$ $(M - Br)^+$ 409.1272; found 409.1276.

5.2.6. 1-{4-[4-(bromomethyl)phenethyl]benzyl}-4-pyrrolidinopyridinium bromide (**26**)

Yield: 60%. M.p. 243–245 °C ^{1}H NMR (400 MHz, CD_3OD) δ 8.16 (d, J = 7.1 Hz, 2H); 7.28–7.19 (m, 6H); 7.11 (d, J = 7.8 Hz, 2H); 6.84 (d, J = 7.1 Hz, 2H); 5.30 (s, 2H); 4.52 (s, 2H); 3.55 (t, J = 6.3 Hz, 4H); 2.91 (m, 4H); 2.12 (q, J = 6.3 Hz, 4H). ^{13}C NMR (75 MHz, CD_3OD) δ 155.20, 144.18, 143.01, 142.96 × 2, 137.25, 133.87, 130.60 × 2, 130.15 × 2, 129.91 × 2, 129.33 × 2, 109.67 × 2, 61.57, 49.71 × 2, 38.34, 38.30, 34.02, 26.12 × 2. HRMS (m/z) calcd for $C_{25}H_{28}N_2Br$ $(M - Br)^+$ 435.1436; found 435.1427.

5.2.7. 1-(4-{4-[4-(bromomethyl)phenyl]butyl}benzyl)-4-(dimethylamino)pyridinium bromide (**27**)

Yield: 64%. M.p. 193–198 °C ^{1}H NMR (400 MHz, CD_3OD) δ 8.20 (d, J = 7.7 Hz, 2H); 7.30–7.21 (m, 6H); 7.12 (d, J = 7.9 Hz, 2H); 6.99 (d, J = 7.7 Hz, 2H); 5.31 (s, 2H); 4.54 (s, 2H); 3.24 (s, 6H); 2.66–2.60 (m, 4H); 1.64–1.60 (m, 4H). ^{13}C NMR (75 MHz, CD_3OD) δ 157.92, 145.13, 144.06, 143.01 × 2, 136.98, 133.46, 130.41 × 2, 130.14 × 2, 129.75 × 2, 129.41 × 2, 109.08 × 2, 61.56, 40.39 × 2, 36.29, 36.25, 34.27, 32.07, 31.98. HRMS (m/z) calcd for $C_{25}H_{30}N_2Br$ $(M - Br)^+$ 437.1593; found 437.1596.

5.2.8. 1-(4-{4-[4-(bromomethyl)phenyl]butyl}benzyl)-4-pyrrolidinopyridinium bromide (**28**)

Yield: 63%. M.p. 180 °C (gel) – 185 °C (foam). ^{1}H NMR (400 MHz, CD_3OD) δ 8.18 (d, J = 7.5 Hz, 2H); 7.30–7.21 (m, 6H); 7.12 (d, J = 7.9 Hz, 2H); 6.84 (d, J = 7.5, 2H); 5.30 (s, 2H); 4.53 (s, 2H); 3.54 (t, J = 6.8 Hz, 4H); 2.72–2.57 (m, 4H); 2.11 (q, J = 6.8 Hz, 4H); 1.62 (m, 4H). ^{13}C NMR (125 MHz, CD_3OD) δ 155.19, 145.19, 144.08, 142.95 × 2, 137.04, 133.52, 130.44 × 2, 130.13 × 2, 129.75 × 2, 129.33 × 2, 109.66 × 2, 61.67, 49.70 × 2, 36.29, 36.26, 34.19, 32.05, 31.96, 26.11 × 2. HRMS (m/z) calcd for $C_{27}H_{32}N_2Br$ $(M - Br)^+$ 463.1749; found 463.1741.

5.3. General procedure for the synthesis of the target compounds

A mixture of adenine (1 equiv.), the corresponding monocationic intermediate (1 equiv.) and K_2CO_3 (2 equiv.) in DMF (4 mL) was microwave-irradiated at a set temperature of 130 °C for 30 min. Solvent was evaporated and the crude product was purified by flash column chromatography using as eluent CH_2Cl_2/methanol (10/0.5→7/3) to afford **8**–**20**. The discrimination between N-9 and N-3 substituted derivatives has been clarified through the HMBC experiment to three bonds.

5.3.1. 1-{4-[(6-amino-9H-purin-9-yl)methyl]benzyl}-4-(dimethylamino)pyridinium bromide (**8**)

Yield: 41%. M.p. 271 °C (decomposition). ^{1}H NMR (400 MHz, CD_3OD) δ 8.19–8.16 (m, 4H); 7.40 (d, J = 8.3 Hz, 2H); 7.35 (d,

J = 8.3 Hz, 2H); 6.97 (d, J = 7.8 Hz, 2H); 5.45 (s, 2H); 5.34 (s, 2H); 3.23 (s, 6H). ^{13}C NMR (125 MHz, CD_3OD) δ 158.02, 157.37, 153.93, 150.70, 143.09 × 2, 142.60, 138.86, 136.15, 129.88 × 2, 129.70 × 2, 120.01, 109.14 × 2, 61.28, 47.62, 40.36 × 2. HRMS (m/z) calcd for $C_{20}H_{22}N_7$ $(M - Br)^+$ 360.1937; found 360.1948. Anal. $C_{20}H_{22}N_7Br \cdot 1.2H_2O$ (C, H, N).

*5.3.2. 1-{4-[(6-amino-9H-purin-9-yl)methyl]benzyl}-4-pyrrolidinopyridinium bromide (**9**)*

Yield: 56%. M.p. >350 °C (decomposition). ^{1}H NMR (300 MHz, DMSO-d_6) δ 8.38 (d, J = 7.5 Hz, 2H); 8.27 (s, 1H); 8.11 (s, 1H); 7.38 (d, J = 8.3 Hz, 2H); 7.35 (d, J = 8.3 Hz, 2H); 7.20 (bs, 2H); 6.86 (d, J = 7.5 Hz, 2H); 5.39 (s, 2H); 5.37 (s, 2H); 3.45 (t, J = 6.4 Hz, 4H); 1.97 (q, J = 6.4 Hz, 4H). ^{13}C NMR (75 MHz, DMSO-d_6) δ 155.92, 152.97, 152.57, 149.36, 141.88 × 2, 140.74, 137.61, 135.33, 128.31 × 2, 128.16 × 2, 118.64, 108.54 × 2, 58.91, 48.28 × 2, 45.75, 24.59 × 2. HRMS (m/z) calcd for $C_{22}H_{24}N_7$ $(M - Br)^+$ 386.2094; found 386.2093. Anal. $C_{22}H_{24}N_7Br \cdot 0.6H_2O$ (C, H, N).

*5.3.3. 1-(4-{4-[(6-amino-9H-purin-9-yl)methyl]phenyl}benzyl)-4-(dimethylamino)pyridinium bromide (**10**)*

Yield: 26%. M.p. >350 °C (decomposition). ^{1}H NMR (400 MHz, DMSO-d_6) δ 8.42 (d, J = 7.1 Hz, 2H); 8.28 (s, 1H); 8.15 (s, 1H); 7.67 (d, J = 7.9 Hz, 2H); 7.62 (d, J = 7.9 Hz, 2H); 7.46 (d, J = 7.9 Hz, 2H); 7.40 (d, J = 7.9 Hz, 2H); 7.20 (bs, 2H); 7.05 (d, J = 7.1 Hz, 2H); 5.42 (s, 2H); 5.41 (s, 2H); 3.18 (s, 6H). ^{13}C NMR (125 MHz, DMSO-d_6) δ 155.99, 155.91, 152.66, 149.46, 142.03 × 2, 140.87, 139.98, 138.80, 136.69, 135.03, 128.65 × 2, 128.21 × 2, 127.25 × 2, 127.03 × 2, 118.68, 107.99 × 2, 58.93, 48.58 × 2, 45.84. HRMS (m/z) calcd for $C_{26}H_{26}N_7$ $(M - Br)^+$ 436.2250; found 436.2240. Anal. $C_{26}H_{26}N_7Br \cdot 1.6H_2O$ (C, H, N).

*5.3.4. 1-(4-{4-[(6-amino-9H-purin-9-yl)methyl]phenyl}benzyl)-4-pyrrolidinopyridinium bromide (**11**)*

Yield: 43%. M.p. 245–246 °C ^{1}H NMR (500 MHz, DMSO-d_6) δ 8.43 (d, J = 7.6 Hz, 2H); 8.30 (s, 1H); 8.14 (s, 1H); 7.66 (d, J = 8.3 Hz, 2H); 7.62 (d, J = 8.3 Hz, 2H); 7.46 (d, J = 8.3 Hz, 2H); 7.40 (d, J = 8.3 Hz, 2H); 7.23 (bs, 2H); 6.91 (d, J = 7.6 Hz, 2H); 5.43 (s, 2H); 5.41 (s, 2H); 3.48 (t, J = 6.7 Hz, 4H); 1.98 (q, J = 6.7 Hz, 4H). ^{13}C NMR (125 MHz, DMSO-d_6) δ 155.99, 153.03, 152.63, 149.45, 142.00 × 2, 140.79, 139.96, 138.77, 136.68, 135.07, 128.55 × 2, 128.17 × 2, 127.23 × 2, 127.01 × 2, 118.60, 108.61 × 2, 59.06, 48.32 × 2, 45.82, 24.64 × 2. HRMS (m/z) calcd for $C_{28}H_{28}N_7$ $(M - Br)^+$ 462.2406; found 462.2426. Anal. $C_{28}H_{28}N_7Br \cdot 0.6H_2O$ (C, H, N).

*5.3.5. 1-(4-{4-[(6-amino-9H-purin-9-yl)methyl]phenethyl}benzyl)-4-(dimethylamino)pyridinium bromide (**12**)*

Yield: 72%. M.p. 163–166 °C ^{1}H NMR (300 MHz, CD_3OD) δ 8.21 (s, 1H); 8.17 (d, J = 7.9 Hz, 2H); 8.11 (s, 1H); 7.25–7.18 (m, 6H); 7.13 (d, J = 8.2 Hz, 2H); 6.98 (d, J = 7.9 Hz, 2H); 5.38 (s, 2H); 5.29 (s, 2H); 3.24 (s, 6H); 2.89 (m, 4H). ^{13}C NMR (75 MHz, CD_3OD) δ 157.97, 157.33, 153.84, 150.68, 144.22, 142.99 × 2, 142.86, 142.60, 135.21, 133.59, 130.60 × 2, 130.15 × 2, 129.34 × 2, 128.76 × 2, 119.96, 109.05 × 2, 61.57, 47.84, 40.38 × 2, 38.29, 38.23. HRMS (m/z) calcd for $C_{28}H_{30}N_7$ $(M - Br)^+$ 464.2563; found 464.2574. Anal. $C_{28}H_{30}N_7Br \cdot 1.2H_2O$ (C, H, N).

*5.3.6. 1-(4-{4-[(6-amino-9H-purin-9-yl)methyl]phenethyl}benzyl)-4-pyrrolidinopyridinium bromide (**13**)*

Yield: 41%. M.p. 203–207 °C ^{1}H NMR (400 MHz, CD_3OD) δ 8.21 (s, 1H); 8.14 (d, J = 7.7 Hz, 2H); 8.10 (s, 1H); 7.27–7.19 (m, 6H); 7.13 (d, J = 7.9 Hz, 2H); 6.83 (d, J = 7.7 Hz, 2H); 5.37 (s, 2H); 5.28 (s, 2H); 3.54 (t, J = 6.8 Hz, 4H); 2.89 (m, 4H); 2.11 (q, J = 6.8 Hz, 4H). ^{13}C NMR (75 MHz, CD_3OD) δ 157.33, 155.13, 153.84, 150.67, 144.16, 142.92 × 2, 142.87, 142.61, 135.20, 133.72, 130.58 × 2, 130.15 × 2, 129.32 × 2, 128.77 × 2, 119.95, 109.64 × 2, 61.58, 49.73 × 2, 47.83, 38.29, 38.24, 26.12 × 2. HRMS (m/z) calcd for $C_{30}H_{32}N_7$ $(M - Br)^+$ 490.2720; found 490.2721. Anal. $C_{30}H_{32}N_7Br \cdot 0.8H_2O$ (C, H, N).

*5.3.7. 1-[4-(4-{4-[(6-amino-9H-purin-9-yl)methyl]phenyl}butyl) benzyl]-4-(dimethylamino)pyridinium bromide (**14**)*

Yield: 54%. M.p. >350 °C (decomposition). ^{1}H NMR (500 MHz, CD_3OD) δ 8.20–8.19 (m, 3H); 8.14 (s, 1H); 7.26 (d, J = 8.1 Hz, 2H); 7.21 (d, J = 8.1 Hz, 2H); 7.18 (d, J = 8.1 Hz, 2H); 7.12 (d, J = 8.1 Hz, 2H); 6.97 (d, J = 7.7 Hz, 2H); 5.38 (s, 2H); 5.31 (s, 2H); 3.23 (s, 6H); 2.61–2.57 (m, 4H); 1.57 (q, J = 3.3, 7.1, 4H). ^{13}C NMR (125 MHz, CD_3OD) δ 157.96, 157.32, 153.84, 150.68, 145.16, 143.89, 143.00 × 2, 142.63, 134.96, 133.40, 130.41 × 2, 129.99 × 2, 129.38 × 2, 128.74 × 2, 119.96, 109.07 × 2, 61.59, 47.84, 40.36 × 2, 36.23, 36.21, 31.93 × 2. HRMS (m/z) calcd for $C_{30}H_{34}N_7$ $(M - Br)^+$ 492.2876; found 492.2877. Anal. $C_{30}H_{34}N_7Br \cdot 1.6H_2O$ (C, H, N).

*5.3.8. 1-[4-(4-{4-[(6-amino-9H-purin-9-yl)methyl]phenyl}butyl) benzyl]-4-pyrrolidinopyridinium bromide (**15**)*

Yield: 26%. M.p. 244 °C (gel) – 259 °C (foam). ^{1}H NMR (500 MHz, CD_3OD) δ 8.21 (s, 1H); 8.16 (d, J = 7.6 Hz, 2H); 8.12 (s, 1H); 7.26–7.17 (m, 6H); 7.12 (d, J = 8 Hz, 2H); 6.83 (d, J = 7.6 Hz, 2H); 5.38 (s, 2H); 5.29 (s, 2H); 3.53 (t, J = 6.8 Hz, 4H); 2.61–2.57 (m, 4H); 2.11 (q, J = 6.8 Hz, 4H); 1.58 (q, J = 7.1 Hz, 4H). ^{13}C NMR (125 MHz, CD_3OD) δ 157.34, 155.14, 153.70, 150.69, 145.15, 143.89, 142.91 × 2, 142.61, 134.96, 133.50, 130.41 × 2, 129.99 x2, 129.32 × 2, 128.73 x2, 119.97, 109.64 x2, 61.64, 49.70 x2, 47.84, 36.23, 36.21, 31.92 x2, 26.12 x2. HRMS (m/z) calcd for $C_{32}H_{36}N_7$ $(M - Br)^+$ 518.3032; found 518.3041. Anal. $C_{32}H_{36}N_7Br \cdot 0.8H_2O$ (C, H, N).

*5.3.9. 1-{4-[(6-amino-3H-purin-3-yl)methyl]benzyl}-4-(dimethylamino)pyridinium bromide(**16**)*

Yield: 24%. M.p. 271 °C (decomposition). ^{1}H NMR (400 MHz, CD_3OD) δ 8.43 (s, 1H); 8.16 (d, J = 7.8 Hz, 2H); 7.88 (s, 1H); 7.46 (d, J = 8.2 Hz, 2H); 7.35 (d, J = 8.2 Hz, 2H); 6.96 (d, J = 7.8 Hz, 2H); 5.60 (s, 2H); 5.34 (s, 2H); 3.23 (s, 6H). ^{13}C NMR (125 MHz, CD_3OD) δ 158.02, 156.81, 153.11, 150.73, 145.68, 143.09 × 2, 137.78, 136.52, 129.85 × 4, 120.99, 109.12 × 2, 61.24, 53.62, 40.32 × 2. HRMS (m/z) calcd for $C_{20}H_{22}N_7$ $(M - Br)^+$ 360.1937; found 360.1935. Anal. $C_{20}H_{22}N_7Br \cdot 0.8H_2O$ (C, H, N).

*5.3.10. 1-(4-{4-[(6-amino-3H-purin-3-yl)methyl]phenyl}benzyl)-4-(dimethylamino)pyridinium bromide (**17**)*

Yield: 23%. M.p. >350 °C (decomposition). ^{1}H NMR (500 MHz, CD_3OD) δ 8.46 (s, 1H); 8.24 (d, J = 7.7 Hz, 2H); 7.94 (s, 1H); 7.66 (d, J = 8.2 Hz, 2H); 7.61 (d, J = 8.2 Hz, 2H); 7.48 (d, J = 8.2 Hz, 2H); 7.45 (d, J = 8.2 Hz, 2H); 7.01 (d, J = 7.7 Hz, 2H); 5.64 (s, 2H); 5.40 (s, 2H); 3.25 (s, 6H). ^{13}C NMR(125 MHz, CD_3OD) δ 158.05, 156.74, 153.00, 150.20, 145.78, 143.11 × 2, 142.57, 141.64, 136.13, 135.39, 129.92 × 2, 129.52 × 2, 128.92 × 2, 128.58 × 2, 120.85, 109.15 × 2, 61.44, 53.76, 40.36 × 2. HRMS (m/z) calcd for $C_{26}H_{26}N_7$ $(M - Br)^+$ 436.2250; found 436.2233. Anal. $C_{26}H_{26}N_7Br \cdot 1.3H_2O$ (C, H, N).

*5.3.11. 1-(4-{4-[(6-amino-3H-purin-3-yl)methyl]phenethyl} benzyl)-4-pyrrolidinopyridinium bromide (**18**)*

Yield: 36%. M.p. 203–207 °C ^{1}H NMR (500 MHz, CD_3OD) δ 8.33 (s, 1H); 8.14 (d, J = 7.4 Hz, 2H); 7.91 (s, 1H); 7.27 (d, J = 7.9 Hz, 2H); 7.23 (d, J = 7.9 Hz, 2H); 7.18 (d, J = 7.9 Hz, 2H); 7.14 (d, J = 7.9 Hz, 2H); 6.83 (d, J = 7.4 Hz, 2H); 5.53 (s, 2H); 5.28 (s, 2H); 3.53 (t, J = 6.6 Hz, 4H); 2.89 (m, 4H); 2.11 (t, J = 6.6 Hz, 4H). ^{13}C NMR (125 MHz, CD_3OD) δ 156.70, 155.21, 153.18, 150.81, 145.48, 144.17, 143.32, 142.91 × 2, 134.05, 133.65, 130.61 × 2, 130.25 × 2, 129.29 × 2, 129.00 × 2, 121.12, 109.63 × 2, 61.66, 53.86, 49.70 × 2, 38.20 × 2, 26.11 × 2. HRMS (m/z) calcd for $C_{30}H_{32}N_7$ $(M - Br)^+$ 490.2720; found 490.2711. Anal. $C_{30}H_{32}N_7Br \cdot 1.3H_2O$ (C, H, N).

*5.3.12. 1-[4-(4-{4-[(6-amino-3H-purin-3-yl)methyl]phenyl}butyl) benzyl]-4-(dimethylamino)pyridinium bromide (**19**)*

Yield: 23%. M.p. >350 °C (decomposition). ^{1}H NMR (500 MHz, CD_3OD) δ 8.39 (s, 1H); 8.19 (d, J = 7.8 Hz, 2H); 7.92 (s, 1H); 7.28 (d, J = 8.1 Hz, 2H); 7.25 (d, J = 8.1 Hz, 2H); 7.19 (d, J = 8.1 Hz, 2H); 7.14 (d, J = 8.1 Hz, 2H); 6.98 (d, J = 7.8 Hz, 2H); 5.54 (s, 2H); 5.30 (s, 2H); 3.24 (s, 6H); 2.62–2.58 (m, 4H); 1.58 (q, J = 7, 4H). ^{13}C NMR (125 MHz, CD_3OD) δ 158.00, 156.69, 153.02, 150.43, 145.66, 145.20, 144.36, 143.01 × 2, 133.85, 133.39, 130.43 × 2, 130.07 × 2, 129.36 × 2, 128.94 × 2, 120.63, 109.07 × 2, 61.61, 53.86, 40.34 × 2, 36.23 × 2, 31.90 × 2. HRMS (m/z) calcd for $C_{30}H_{34}N_7$ $(M - Br)^+$ 492.2876; found 492.2874. Anal. $C_{30}H_{34}N_7Br \cdot 1.3H_2O$ (C, H, N).

*5.3.13. 1-[4-(4-{4-[(6-amino-3H-purin-3-yl)methyl]phenyl}butyl) benzyl]-4-pyrrolidinopyridinium bromide (**20**)*

Yield: 38%. M.p. 244 °C (gel) – 259 °C (foam). ^{1}H NMR (500 MHz, CD_3OD) δ 8.38 (s, 1H); 8.16 (d, J = 7.6 Hz, 2H); 7.92 (s, 1H); 7.28 (d, J = 8 Hz, 2H); 7.25 (d, J = 8 Hz, 2H); 7.17 (d, J = 8 Hz, 2H); 7.12 (d, J = 8 Hz, 2H); 6.82 (d, J = 7.6 Hz, 2H); 5.54 (s, 2H); 5.29 (s, 2H); 3.52 (t, J = 6.8 Hz, 4H); 2.60–2.56 (m, 4H); 2.10 (q, J = 6.8 Hz, 4H); 1.57 (q, J = 7, 4H). ^{13}C NMR (125 MHz, CD_3OD) δ 156.65, 155.14, 153.01, 150.77, 145.61, 145.11, 144.35, 142.92 × 2, 133.83, 133.49, 130.39 × 2, 130.06 × 2, 129.34 × 2, 128.97 × 2, 120.92, 109.65 x2, 61.64, 53.86, 49.70 x2, 36.21 x2, 31.86 x2, 26.11 x2. HRMS (m/z) calcd for $C_{32}H_{36}N_7$ $(M - Br)^+$ 518.3032; found 518.3039. Anal. $C_{32}H_{36}N_7Br \cdot 1.2H_2O$ (C, H, N).

5.4. Biological assays

[Methyl-^{14}C]choline chloride (55 mCi/mmol) was supplied by Perkin Elmer (Massachusetts, USA). Fetal bovine serum (FBS) was from The Cell Culture Company (Pasching, Austria). Minimal essential medium (MEM) was from Sigma–Aldrich (Madrid, Spain). Thin-layer chromatography (TLC) plates of Silica Gel 60 A was acquired from Whatman (Kent, UK). Microwell plates and culture dishes were obtained from NuncTM (Langenselbold, Germany). All other reagents were of analytical grade. The human hepatoma HepG2 cell line was from The European Collection of Animal Cell Cultures (Salisbury, UK). Cells were cultured in MEM containing 10% heat-inasctivated FBS, supplemented with 2 mM L-glutamine, 1% nonessential amino acids, 100 U/ml penicillin and 100 μg/ml streptomycin. Cells were grown in a humidified atmosphere with 5% CO_2 at 37 °C and were subcultured at a 1:10 ratio once a week. Cells were plated on tissue-culture dishes at a density of 5 x 104 cells/cm^2 and maintained in culture at approximately 70% confluence. Cytosol was obtained as described [23] with minor modifications. Briefly, HepG2 cells were seeded onto 6-well dishes and maintained in MEM containing 10% FBS until confluence. Then, cells were scraped into ice-cold 275 mM Tris (pH 8.5). Cells in suspension were sonicated for 3 s with a microprobe in an ice bath, and the homogenate was centrifuged immediately at 12000 g for 5 min at 4 °C. After centrifugation the cell supernatant was immediately frozen in liquid nitrogen and stored at −80 °C until use.

5.4.1. Choline kinase inhibition

ChoK activity was assayed by measurement of the rate of incorporation of ^{14}C from [methyl-^{14}C]choline into phosphocholine. Briefly, the final reaction mixture contained 100 mM Tris (pH 8.5), 10 mM $MgCl_2$, and 10 mM ATP, approximately 50 μg of cytosolic protein and different amounts of ChoK inhibitors. The reaction was initiated with 1 mM [methyl-^{14}C]choline (4500 dpm/nmol) and it was incubated at 37 °C for 20 min, being the final volume of 50 μl. The assay was stopped by immersion of the reaction tubes in boiling water for 3 min and protein precipitate was removed by centrifugation at 12000 g for 3 min. Aliquots of the supernatant were applied to the origin of Silica Gel plates in the presence of phosphocholine (0.1 mg) and choline (0.1 mg) as carriers. The chromatography was developed in methanol/0.6% NaCl/28% NH_4OH in water (50:50:5, v/v/v) as solvent. Phosphocholine was visualized under exposure to iodine vapor and the corresponding spot was scraped and transferred to scintillation vials for measurement of radioactivity by a Beckman 6000-TA (Madrid, Spain) liquid scintillation counter.

5.4.2. Cell proliferation

HepG2 cells were seeded onto 96-well plates (10 000 cells/well) and maintained in MEM containing 10% FBS for 24 h. Then, the culture medium was replaced with fresh medium/10% FBS and the cells were incubated for 24 h in the absence or presence of different amounts of ChoK inhibitors before analyses. The antiproliferative effect of the distinct compounds was assessed by the crystal violet-staining assay using a cell number-based standard curve. The medium was removed and the cells were fixed by addition of 100 μl of a 1.1% glutaraldehyde solution. After shaking (50 rpm for 15 min), plates were washed eight times with ultrapure water. Plates were air-dried and stained by addition of 200 μl of a 0.1% solution of crystal violet dissolved in water. After shaking (30 rpm for 20 min), the dye was removed and plates were extensively washed with deionized water. Samples were air-dried prior to dye solubilisation in 100 μl of 10% acetic acid. The absorbance of crystal violet in each well was measured at a wavelength of 590 nm directly in plates using a microplate reader.

5.5. Molecular modeling and docking studies

Molecular modeling studies were performed by using Sybyl program [26]. Crystal structure of human ChoKα1 in complex with **HC-3** was obtained from the Protein Data Bank (PDB id: 3G15). This structure contains a homodimeric protein, and Chain A was chosen for docking calculations since in Chain B there are more missing residues. All water molecules and unknown residues were deleted, and only ADP and **HC-3** were conserved in order to define the binding sites.

Protein was refined by using the Structure Preparation Tool module of Sybyl. Missing side chains of those residues situated far away from the binding sites were added, and protein N-terminal and C-terminal were fixed with ACE and NME, respectively. Hydrogens and charges were also added and protonation type of Glu, Asp, Gln and Asp was analyzed and fixed. Hydrogen orientations were also checked in order to maintain intramolecular hydrogen bonds into the protein. Finally, ADP and **HC-3** atom types and connectivity were carefully checked to assure the correction of these molecules.

Ligands were constructed from standard fragments of the Libraries of the Sybyl program. As described previously [16], a new type of atom was necessary to define in order to build the molecules: N.ar4, the quaternary nitrogen of the pyridinium fragments. Additional parameters were also developed from *ab initio* calculations to optimize the geometry of these molecules [16]. Charges were calculated by means of Gaussian Program [27], and optimizations were tackled using the BFGS method.

The Surflex-Dock [28] module implemented in the Sybyl program was used for docking studies. Surflex-Dock Protomol was prepared using both ADP and HC-3 ligands inserted into the 3G15 crystal structure, with a threshold value of 0.5 and a Bloat of 0 A. Surflex-Dock GeomX (SFXC) protocol was used, the search grid was expanded in 3 A, 50 additional starting conformation were used for each molecule and 30 conformations per fragment. Results were analyzed using Sybyl program and the most stable pose for each

molecule was chosen as the preferred one inside the ChoK enzyme. Figures were built using the PyMOL program [29].

Acknowledgments

We thank the "Consejería de Innovación, Ciencia y Empresa, Junta de Andalucía" (Excellence Research Project no. P07-CTS-03210) and the " Ministerio de Ciencia e Innovación" (Project no. SAF2009-11955) for the financial support. The award of grants from the "Ministerio de Educación" to B R–R. and P.R-M is gratefully acknowledged. We thank Xiomara Gálvez for her technical support.

Appendix. Supplementary material

Supplementary material associated with this article can be found, in the online version, at doi:10.1016/j.ejmech.2012.01.050.

References

[1] C. Aoyama, H. Liao, K. Ishidate, Structure and function of choline kinase isoforms in mammalian cells, Prog. Lipid. Res. 43 (2004) 266–281.
[2] A. Ramírez de Molina, R.A. González, J.C. . Lacal, From Ras signalling to ChoK inhibitors: a further advance in anticancer drug design, Cancer Lett. 206 (2004) 137–148.
[3] S. Janardhan, P. Srivani, G.N. Sastry, Choline kinase: an important target for cancer, Curr. Med. Chem. 13 (2006) 1169–1186.
[4] H.R. Alcoceba, L. Saniger, J. Campos, M.C. Nunez, F. Khaless, M.A. Gallo, A. Espinosa, J.C. Lacal, Choline kinase inhibitors as a novel approach for antiproliferative drug design, Oncogene 15 (1997) 2289–2301.
[5] A. Ramírez de Molina, D. Gallego-Ortega, J. Sarmentero, M. Bañez-Coronel, Y. Martin-Cantalejo, J.C. . Lacal, Choline kinase is a novel oncogene that potentiates RhoA-induced carcinogenesis, Cancer Res. 65 (2005) 5647–5653.
[6] J.C. Lacal, J. Moscat, S.A. Aaronson, Novel source of 1,2-diacylglycerol elevated in cells transformed by Ha-ras oncogene, Nature 330 (1987) 269–272.
[7] K. Glunde, T. Shah, P.T. . Winnard Jr., V. Raman, T. Takagi, F. Vesuna, D. Artemov, Z.M. Bhujwalla, Hypoxia regulates choline kinase expression through hypoxia-inducible factor-1 alpha signaling in a human prostate cancer model, Cancer Res. 68 (2008) 172–180.
[8] A. Ramírez de Molina, A. Rodríguez-Gonzalez, R. Gutierrez, L. Martinez-Pineiro, J. Sanchez, F. Bonilla, R. Rosell, J. Lacal, Overexpression of choline kinase is a frequent feature in human tumor-derived cell lines and in lung, prostate, and colorectal human cancers, Biochem. Biophys. Res. Commun. 296 (2002) 580–583.
[9] G. Eliyahu, T. Kreizman, H. Degani, Phosphocholine as a biomarker of breast cancer: molecular and biochemical studies, Int. J. Cancer 120 (2007) 1721–1730.
[10] M. Bañez-Coronel, A. Ramirez de Molina, A. Rodríguez-González, J. Sarmentero, M.A. Ramos, M.A. García-Cabezas, L. García-Oroz, J.C. Lacal, Choline kinase alpha depletion selectively kills tumoral cells, Curr. Cancer Drug Targets 8 (2008) 709–719.
[11] A. Ramírez de Molina, J. Sarmentero-Estrada, C. Belda-Iniesta, M. Taron, V. Ramirez de Molina, P. Cejas, M. Skrzypski, D. Gallego-Ortega, J. De Castro, E. Casado, M.A. García-Cabezas, J.J. Sánchez, M. Nistal, R. Rosell, M. González-Barón, J.C. . Lacal, Expression of choline kinase alpha to predict outcome in patients with early-stage non-small-cell lung cancer: a retrospective study, Lancet Oncol. 8 (2007) 889–897.
[12] A. Conejo-García, M. Bañez-Coronel, R. Sánchez-Martín, A. Rodríguez-González, A. Ramos, A. Ramírez de Molina, A. Espinosa, M.A. Gallo, J. Campos, J.C. Lacal, Influence of the linker in bispyridinium compounds on the inhibition of human choline kinase, J. Med. Chem. 47 (2004) 5433–5440.
[13] R. Sanchez-Martín, J.M. Campos, A. Conejo-García, O. Cruz-López, M. Bañez-Coronel, A. Rodríguez-González, M.A. Gallo, J.C. Lacal, A. Espinosa, Symmetrical bis-quinolinium compounds: new human choline kinase inhibitors with antiproliferative activity against the ht-29 cell line, J. Med. Chem. 48 (2005) 3354–3363.
[14] A. Conejo-García, J. Campos, R.M. Sanchez, A. Rodríguez-Gonzalez, J.C. Lacal, M.A. Gallo, A. Espinosa, Choline kinase inhibitory effect and antiproliferative activity of new 1,1',1''-(benzene-1,3,5-triylmethylene)tris {4-[(disubstituted)amino]pyridinium} tribromides, Eur. J. Med. Chem. 38 (2003) 109–116.
[15] A. Conejo-García, J.M. Campos, R.M. Sánchez-Martín, M.A. Gallo, A. Espinosa, Bispyridinium cyclophanes: novel templates for human choline kinase inhibitors, J. Med. Chem. 46 (2003) 3754–3757.
[16] A. Conejo-García, J.M. Campos, A. Entrena, R.M. Sánchez-Martín, M.A. Gallo, A. Espinosa, Conformational dynamics of a bispyridinium cyclophane, J. Org. Chem. 68 (2003) 8697–8699.
[17] A. Conejo-García, J. Campos, C. Eder, A. Entrena, M.A. Gallo, A. Espinosa, Synthesis and NMR studies on a C3-symmetrical triquinolina triscationic bicyclophane, J. Org. Chem. 70 (2005) 5748–5751.
[18] L. Milanese, A. Espinosa, J.M. Campos, M.A. Gallo, A. Entrena, Insight into the inhibition of human choline kinase: homology modelling and molecular dynamics simulations, ChemMedChem. 1 (2006) 1216–1228.
[19] D. Peisach, P. Gee, C. Kent, Z. Xu, The crystal structure of choline kinase reveals a eukaryotic protein kinase fold, Structure 11 (2003) 703–713.
[20] E. Malito, N. Sekulic, W.C. Too, M. Konrad, A. Lavie, Elucidation of human choline kinase crystal structures in complex with the products ADP or phosphocholine, J. Mol. Biol. 364 (2006) 136–151.
[21] H.A. Staab, M. Haenel, Synthesen won [2.2](4,4')biphenylophan,[2.2](2,7) phenanthrenophan und [2](4,4')biphenylo[2](2, 7)phenanthrenophan, Chem. Ber. 106 (1973) 2190–2202.
[22] D.J. Cram, H. Steinberg, Macro rings. I. Preparation and spectra of the paracyclophanes, J. Am. Chem. Soc. 73 (1951) 5691–5704.
[23] J.M. Jiménez-López, M.P. Carrasco, J.L. Segovia, C. Marco, Hexadecylphosphocholine inhibits phosphatidylcholine biosynthesis and the proliferation of HepG2 cells, Eur. J. Biochem. 269 (2002) 4649–4655.
[24] B.S. Hong, A. Allali-Hassani, W. Tempel, P.J. . Finerty Jr., F. MacKenzie, S. Dimov, M. Vedadi, H.-W. Park, Crystal structures of human choline kinase isoforms in complex with hemicholinium-3, J. Biol. Chem. 285 (2010) 16330–16340.
[25] D. Gallego-Ortega, T. Gómez del Pulgar, F. Valdés-Mora, A. Cebrián, J.C. Lacal, Involvement of human choline kinase alpha and beta in carcinogenesis: a different role in lipids metabolism and biological functions, Adv. Enzym. Regul. 51 (2011) 183–194.
[26] SYBYL-X 1.2, Tripos International, 1699 South Hanley Rd., St. Louis, Missouri, 63144, USA. http://www.tripos.com
[27] Gaussian, Inc., C.T. Wallingford.http://www.gaussian.com (2004).
[28] A.N. Jain, Surflex-Dock 2.1: robust performance from ligand energetic modeling, ring flexibility, and knowledge-based search, J. Comput. Aided Mol. Des. 21 (2007) 281–306.
[29] The PyMOL Molecular Graphics System, Version 1.4, Schrödinger, LLC.